JOURNAL OF MATERIALS SCIENCE 23 (1988) 1018–1023

An XPS and reduction study of $PrCoO_3$

J. L. G. FIERRO, M. A. PEÑA, L. GONZÁLEZ TEJUCA*
Instituto de Catálisis y Petroleoquímica, C.S.I.C., Serrano 119, 28006 Madrid, Spain

The perovskite-type oxide $PrCoO_3$ has been studied by means of X-ray photoelectron spectroscopy (XPS), reduction in H_2 and X-ray diffraction. Two types of oxygen were detected: lattice oxygen (binding energy = 528.4 eV) and adsorbed oxygen (binding energy = 530.9 eV). The increase in relative intensity of the peak corresponding to the latter species after reduction of $PrCoO_3$ to $3e^-$ per molecule is assigned to the formation of hydroxyl groups. Temperature-programmed reduction (TPR) results showed two reduction steps: to $1e^-$ per molecule ($Co^{3+} \rightarrow Co^{2+}$) at 475 to 635 K, and to $3e^-$ per molecule ($Co^{2+} \rightarrow Co^0$) at 725 to 815 K. Reduction in the first and second steps occurs according to the contracting sphere model and the nucleation mechanism, respectively. Reduction of Co^{3+} to Co^{2+} causes minimal structural changes in the perovskite. Reduction to $3e^-$ per molecule yielded Pr_2O_3 and metallic cobalt. After this reduction and reoxidation at 973 K, the perovskite structure was regained. By XPS and TPR it was shown that $PrCoO_3$ is more easily reducible than $LaCoO_3$. It is concluded that the cation in the A position of the structure plays a significant role in the bulk and surface properties of $LnCoO_3$ (Ln, lanthanide elements) oxides.

1. Introduction

Praseodymium oxide together with terbium oxide exhibit maxima of catalytic activity for H_2 [1] and NO [2] oxidation and also for the initial rate of isotopic exchange of oxygen from the oxide lattice with molecular oxygen [1], within the series of oxides of rare-earth elements. The rate of oxygen exchange in praseodymium oxide (Pr_6O_{11}) is very similar to that of cobalt monoxide and manganese dioxide which are known to have a high catalytic activity for oxidation [1]. From this it can be inferred that the high oxidation activity is directly related with the high oxygen mobility in these oxides. Supporting this assumption, Futai *et al.* [3] found a correlation amongst the oxygen binding energy, the reducibility (which can be considered as a measure of oxygen mobility) and the catalytic activity for CO oxidation in perovskite-type oxides $LnCoO_3$ (Ln, rare-earth element). These findings are in agreement with the results on this series of oxides reported by Arakawa *et al.* [4].

$LaCoO_3$ exhibits the highest catalytic activity for oxidation of CO, propene and isobutene within the series of $LaMO_3$ oxides (M, first-row transition metal) [5, 6]. This catalytic activity should be higher for $PrCoO_3$ since the oxygen binding energy in this oxide is lower than that for $LaCoO_3$ [3]. In this work attention is paid to the reactivity of oxygen in the praseodymium–cobalt perovskite. By means of X-ray photoelectron spectroscopy (XPS), two different types of oxygen were identified and their evolution in the reduced sample was studied. Also gravimetric measurements of reduction at programmed temperature and in isothermal conditions were carried out. These results are compared with those of $LaCoO_3$ and some considerations about the role of the cation in the A position of the perovskite structure are made.

2. Experimental procedure

$PrCoO_3$ was prepared by amorphous citrate decomposition as described previously [7]. Briefly, citrates were precipitated from an equimolecular solution of metal nitrates ($Co(NO_3)_2 \cdot 6H_2O$, Riedel-de-Haën) and $Pr(NO_3)_3 \cdot 5H_2O$, Fluka AG) and citric acid (Merck). The precursor so obtained was calcined in air at 973 K for 4 h. The resulting perovskite has a BET specific surface area (N_2 cross-sectional area $= 0.162\,nm^2$) of $9.0\,m^2\,g^{-1}$. Its X-ray diffraction pattern is given in Fig. 8a below. H_2 and helium were both 99.995% pure.

X-ray photoelectron spectra were obtained by means of a Leybold Heraeus LHS 10 electron spectrometer with a hemispherical energy analyser and a magnesium-anode X-ray source ($h\nu$ = 1253.6 eV) operated at 12 kV and 10 mA. The spectrometer was interfaced to a data acquisition system which allowed accumulation of spectra. Either 20 or 50 eV energy regions of the photoelectrons of interest were recorded at a 50 eV spectrometer pass energy. This was chosen as a compromise enabling one to attain acceptable energy resolution within reasonable data acquisition times. All binding energies (BE) were referenced to the C1s photoemission at 284.6 eV. The samples were pressed at $3 \times 10^5\,kN\,m^{-2}$ into a small cylindrical holder which was subsequently fixed to a long support-rod in the spectrometer. The pressure in the turbo-pumped analysis chamber was below

*To whom correspondence should be addressed.

0022–2461/88 $03.00 + .12

7×10^{-9} torr (1 torr = 133.3 N m^{-2}) during data acquisition. Temperature-programmed reduction (TPR) was carried out in a Cahn microbalance operated to an accuracy of 10 μg. A 40 mg sample was first heated at 4 K min^{-1} up to 800 K in a helium flow. After cooling to room temperature (r.t.) under helium, it was heated again (as above) in an H_2 flow. For isothermal reduction the sample was first heated at 4 K min^{-1} from r.t. to the desired temperature in a helium flow. After stabilization of the temperature, the reduction was effected in an H_2 flow. The helium or H_2 flow rates were, in all cases, 90 cm^3 min^{-1}. The weight of the sample was taken as a measurement of its reduction degree.

X-ray diffractograms were obtained by means of a Philips PW1716/30 diffractometer using Cu$K\alpha$ radiation and a nickel filter. The samples were cooled down from reduction or sintering temperature to r.t. in H_2 or helium.

3. Results and discussion

3.1. XPS results

XP spectra of the O1s photoemission levels of the as-prepared (oxidized) $PrCoO_3$ and of the sample after undergoing a reduction of 3e$^-$ per molecule (in the TPR experiment, Fig. 2 below) are given in Fig. 1. They include two well-defined peaks at 528.4 and 530.9 eV, the relative intensity of the latter being higher in the reduced sample. In Table I, the O1s photoemission levels of some simple and mixed oxides are given [8–12]. While the peak at lower BE is assigned to lattice oxygen, the peak at higher BE is generally assigned to adsorbed O^- or OH^- although in some cases formation of a surface carbonate was proposed. In $LaMO_3$ oxides, the cation in the A position is strongly basic and this may favour the adsorption of H_2O or CO_2 from the atmosphere. The relative intensity of the O1s peak at higher BE in outgassed (at 773 K) $LaCoO_3$ [13] was smaller than that recorded for a non-pumped sample [11]. On the other hand, the relative intensity increased remarkably after reduction of this oxide at 673 K and higher temperatures [13]. This result is similar to that observed for $PrCoO_3$ (Fig. 1), and suggests that the peak at 530.9 eV is associated with reduction of the perovskite and subsequent formation of praseodymium hydroxide in the presence of the water generated in the reduction process. Thus, the hydroxyl groups of the hydroxide should be responsible for the increase in relative intensity of this peak in reduced $PrCoO_3$ (Fig. 1b). It should be noted that this intensity increase in reduced $PrCoO_3$ was found to be much more pronounced than that observed in $LaCoO_3$ [13], indicating a more profound reduction (effected at 798 K for $PrCoO_3$ and at 773 K for $LaCoO_3$) in the former oxide. This is consistent with the known fact that the stability of ABO_3 oxides increases with the size of the cation in the A position [14].

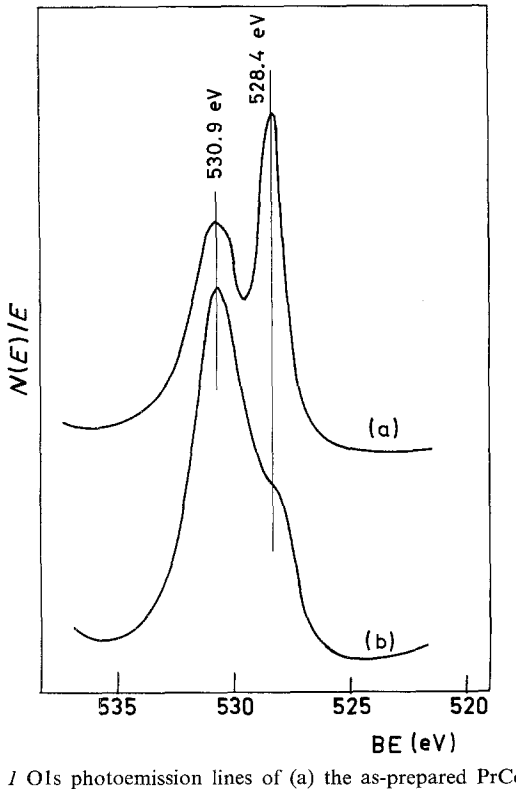

Figure 1 O1s photoemission lines of (a) the as-prepared $PrCoO_3$ and (b) the reduced (to 3e$^-$ per molecule) sample.

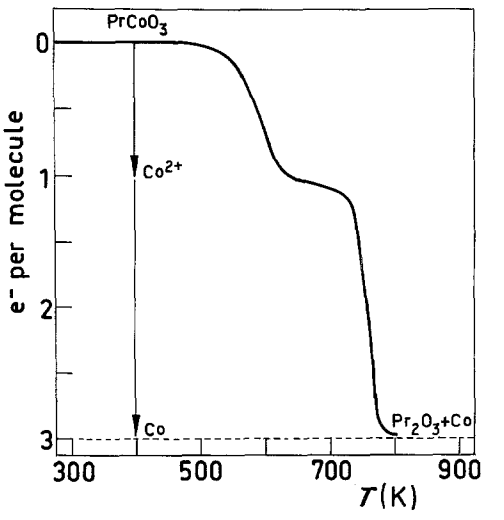

Figure 2 Temperature-programmed reduction of $PrCoO_3$. 90 cm^{-3} min^{-1} H_2 flow rate; 4 K min^{-1} heating rate.

3.2. Temperature-programmed reduction

The TPR diagram of $PrCoO_3$ in terms of e$^-$ per molecule (1e$^-$ per molecule would correspond to reduction of Co^{3+} to Co^{2+}) against temperature is given in

TABLE I O1s photoemission levels in oxides

Compound	BE (eV)	Assignation*	Reference
$LaCoO_3$	Higher BE	a : oxygen	[8]
	Lower BE	l : oxygen	
$LaCoO_3$	531.5	carbonate	[9]
	528.5	l : oxygen	
$La_{1-x}Sr_xCoO_3$	530.2 to 531.4	a : oxygen	[10]
	528.2	l : oxygen	
$LaMO_3$	531.4 to 532.6	a : oxygen or OH^-	[11]
	529.7 to 530.0	l : oxygen	
Co_3O_4	531	a : H_2O or OH^-	[12]
	529.6	l : oxygen	
NiO	531.4	a : O^-	[12]
	Lower BE	l : oxygen	
$PrCoO_3$	530.9	a : oxygen or OH^-	This work
	528.4	l : oxygen	

*a, adsorbed; l, lattice.

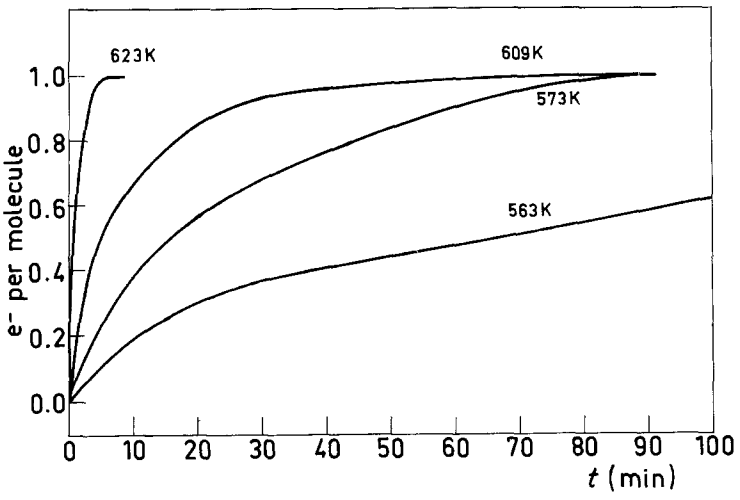

Figure 3 Isothermal reduction of $PrCoO_3$ in the first reduction step (to $1e^-$ per molecule). 90 cm^3 min^{-1} H_2 flow rate; 4 K min^{-1} heating rate.

Fig. 2. Two reduction steps are observed. The first one of the $1e^-$ per molecule takes place between 475 and 635 K; the second one of $3e^-$ per molecule occurs between 725 and 815 K. Similar reduction steps were found for $LaCoO_3$ [15] and $LaNiO_3$ [16]. However, Crespin *et al.* [17] and Levitz *et al.* [18] identified divalent and monovalent nickel phases in reduced $LaNiO_3$. Futai *et al.* [3], measuring the H_2 consumption as a function of the reduction temperature, observed two reduction steps for $PrCoO_3$, although at higher temperatures (maxima for the rate of weight loss would be situated at 650 and 860 K) than those measured in this work. This may be due to the rather different experimental conditions used by these authors (heating rate, 9 K min^{-1}, and a flow of 25 cm^3 min^{-1} (10% H_2 + 90% N_2)). The temperature for reduction levels of $1e^-$ and $3e^-$ per molecule in $PrCoO_3$ (Fig. 2) are lower than those needed for reduction of $LaCoO_3$ (720 and 890 K, respectively) [15]. This also indicates that the lanthanum perovskite is more stable in an H_2 atmosphere than the praseodymium perovskite.

3.3. Kinetics of reduction

Kinetic experiments of reduction in isothermal conditions were carried out at temperatures of 563 to 623 K and 716 to 784 K within the intervals where the first and second steps of reduction take place. The plots of degree of reduction in e^- per molecule against t (time) corresponding to the first step are given in Fig. 3. It is seen that the reduction rate decreases continuously with time, indicating that the reduction process occurs according to the contracting sphere model (an initial fast nucleation and a continuous decrease of the oxidized $PrCoO_3$ grains) [19]. This type of reduction is described by the Mampel intermediate law

$$1 - (1 - \alpha)^{1/n} = kt + b \qquad (1)$$

where k and b are temperature-dependent constants; α is here defined as 10^{-2} % reduction. This equation usually holds over the middle range of α values [20]. An expression similar to Equation 1 may be derived assuming that the reduction process is controlled by the chemical reaction at the interface $PrCoO_3$–reduced phase (not by H_2 diffusion to the interface) [19]. The linear plots of this equation for $n = 3$, $[1 - (1 - \alpha)^{1/3}]$ against t (surface nucleation and advance of the interface towards the centre of the assumed spherical particles), are given in Fig. 4. The experimental results are satisfactorily described for α values between 0.35 to 0.50 (lower limit) and 1 (upper limit), the linearity range being wider for lower reduction temperatures. Linear fits were also obtained for $n = 2$ (two-dimensional growth) although in this case Equation 1 describes the experimental results over a narrower range of α values. The activation energy E_a was calculated by means of an Arrhenius plot of $\ln(1/t_{0.5})$ against $1/T$ ($t_{0.5}$ is the time needed to attain a reduction of $0.5e^-$ per molecule, which is the mean value between the initial and final degrees of reduction) (Fig. 5a). E_a was found to be 170 kJ mol^{-1}.

The kinetic curves for the second reduction step (from $1e^-$ to $3e^-$ per molecule) are given in Fig. 6. They have a sigmoidal shape which indicates that

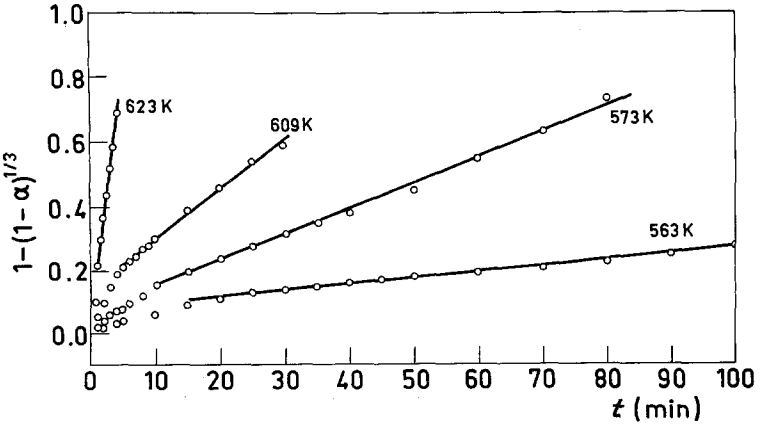

Figure 4 Linear plots of the Mampel intermediate law for the first reduction step.

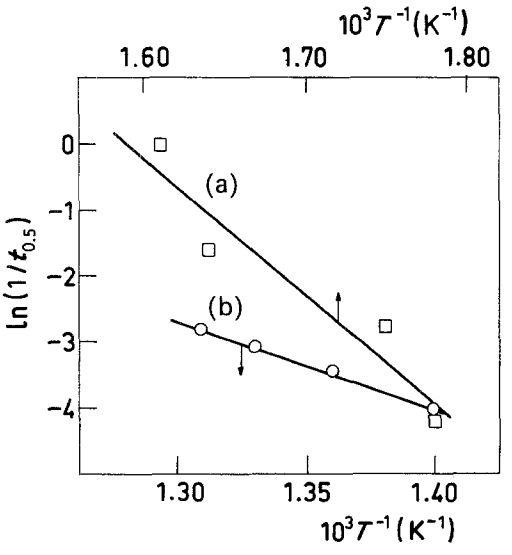

Figure 5 Arrhenius plots of $\ln(1/t_{0.5})$ against $1/T$. $t_{0.5}$, time needed for reduction of $PrCoO_3$ to (a) $0.5e^-$ or (b) $2e^-$ per molecule.

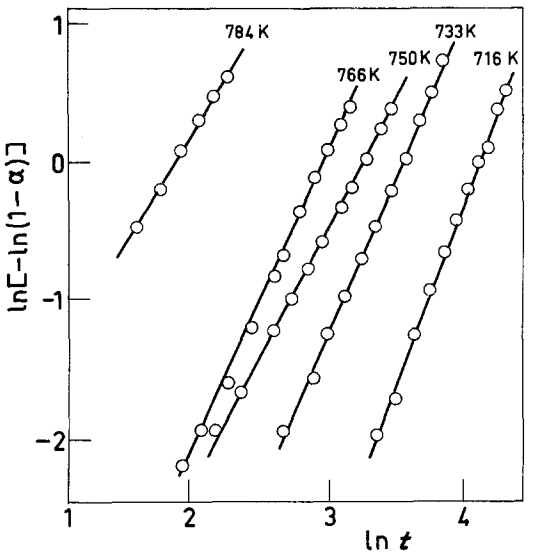

Figure 7 Linearized plots of the Avrami–Erofeev equation for the second reduction step.

reduction occurs through a nucleation mechanism [19]. These kinetic data were fitted to the Avrami–Erofeev equation

$$1 - \alpha = \exp(-kt^n) \quad (2)$$

α and k have similar meanings to those given for Equation 1 [20]. Linearized plots of $\ln[-\ln(1-\alpha)]$ against $\ln t$ are depicted in Fig. 7. From the slope of these lines a mean value of $n = 2.1$ was calculated. This would correspond to a two-dimensional growth of the nuclei. The activation energy for this reduction process, obtained from a plot of $\ln(1/t_{0.5})$ against $1/T$ (where $t_{0.5}$ is the time needed for reduction to $2e^-$ per molecule) (Fig. 5b) was $110\,kJ\,mol^{-1}$.

3.4. X-ray diffraction

A series of X-ray diffraction patterns was obtained to identify the chemical species produced after reduction and reoxidation of $PrCoO_3$. These are given in Fig. 8. Fig. 8a belongs to the as-prepared perovskite. The pattern obtained after reduction to $1e^-$ per molecule showed only peaks of $PrCoO_3$, although they were less intense than those of the starting (fully oxidized) sample. It appears that the concentration of oxygen vacancies produced in the first reduction step (0.5 anion vacancies per molecule) does not destroy the perovskite structure. After reoxidation (973 K, 1 h, air) a spectrum equivalent to that in Fig. 8a was obtained. The pattern of reduced (to $3e^-$ per molecule) $PrCoO_3$ (Fig. 8b) included peaks of praseodymium sesquioxide (B) and metallic cobalt (C). By reoxidation (as above), cobalt is oxidized to Co_3O_4; this is followed by full reaction of simple oxides to perovskite as shown by the pattern in Fig. 8c. However, after reduction to $3e^-$ per molecule, sintering in $90\,cm^3\,min^{-1}$ He at 1123 K for 1 h and reoxidation, only partial reaction of simple oxides to perovskite occurred. This is shown in Fig. 8d where intense peaks of Pr_6O_{11} (D) and Co_3O_4 (E) besides peaks of $PrCoO_3$ (A) were identified. Formation of the perovskite after reduction to $3e^-$ per molecule (with no sintering treatment) and reoxidation were also reported for $LaCoO_3$ [15] and $LaNiO_3$ [16].

Table II gives particle sizes (d) as calculated by the Debye–Scherrer equation $d = K\lambda/\beta \cos\theta$ (K = constant which was taken as 0.9; λ = wavelength of the X-rays used; β = broadening of the spectral line chosen calculated by the equation $\beta^2 = B^2 - b^2$ where B is the measured linewidth and b the width measured under the same experimental conditions with a sample of SiO_2 of a particle size larger than 100 nm; θ = diffraction angle of the line considered). Data are

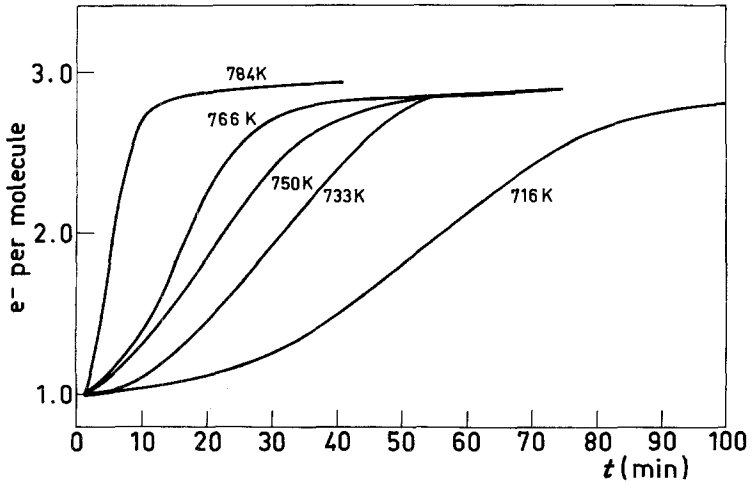

Figure 6 Isothermal reduction of $PrCoO_3$ in the second reduction step (to $3e^-$ per molecule). $90\,cm^3\,min^{-1}$ H_2 flow rate; $4\,K\,min^{-1}$ heating rate.

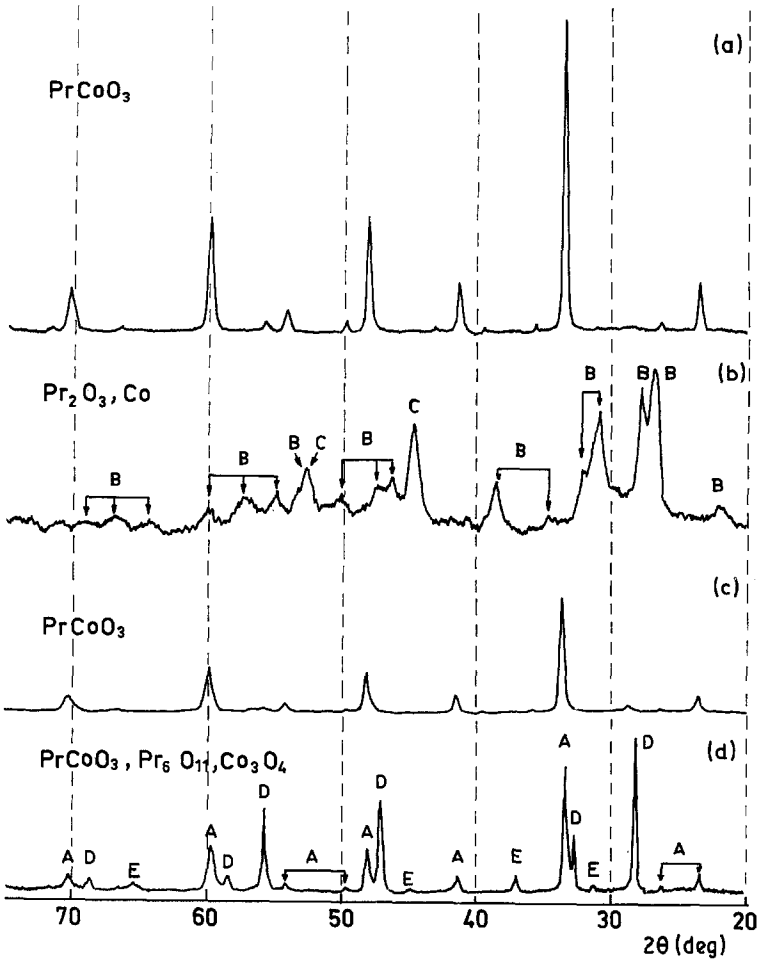

Figure 8 X-ray diffraction patterns of reduced and oxidized samples: (a) as-prepared $PrCoO_3$; (b) after reduction to $3e^-$ per molecule; (c) after reduction to $3e^-$ per molecule and reoxidation (973 K, 1 h, air); (d) after reduction to $3e^-$ per molecule, heating in helium (1123 K, 1 h) and reoxidation (973 K, 1 h, air). (A) $PrCoO_3$; (B) Pr_2O_3; (C) Co; (D) Pr_6O_{11}; (E) Co_3O_4.

given for $PrCoO_3$, simple oxides and metallic cobalt, produced after reduction, sintering in helium and reoxidation as described above. For the starting perovskite a particle size of 33.6 nm was determined. After reduction to $1e^-$ per molecule and reoxidation, the particle size of $PrCoO_3$ remained constant. This result, together with the corresponding diffraction pattern, seems to indicate that reduction in the first step causes minimal structural and textural changes in the perovskite. The particle sizes of Pr_2O_3 and metallic cobalt which are formed in the second reduction step were 11.2 and 10.3 nm, respectively (cobalt was found to be better dispersed on a matrix of La_2O_3 since no X-ray diffraction lines of the metal were observed after reduction of $LaCoO_3$ to $3e^-$ per molecule [15]). These not too high values of d favour the oxidation of cobalt and reaction of Co_3O_4 with Pr_2O_3 to form $PrCoO_3$. Reduction in these conditions is fully reversible, though the perovskite appears to be less crystalline than the starting sample (cf. peak intensity in Figs 8a and c) similarly to that observed for $LaCoO_3$ [15]. However, after reduction to $3e^-$ per molecule, sintering in helium and reoxidation, Pr_6O_{11} of $d = 39.1$ nm and Co_3O_4 of $d = 23.1$ nm are formed. These large particle sizes prevent the complete reaction of the oxides at 973 K and their full conversion to perovskite (Fig. 8d).

3.5. Concluding remarks

The behaviour of $PrCoO_3$ in an H_2 atmosphere is similar to that observed for $LaCoO_3$ [15] in that both oxides exhibited two reduction steps being operative,

TABLE II Particle sizes (d), calculated by the Debye–Scherrer equation, after reduction, sintering in helium and oxidation treatments of $PrCoO_3$*

Treatment†	Chemical species	Crystallographic plane and structure	B (deg)	d (nm)
As-prepared	$PrCoO_3$	(2 2 0), cubic	0.30	33.6
Reduction to $3e^-$ per molecule	Pr_2O_3	(1 1 1), monoclinic	0.75	11.2
Reduction to $3e^-$ per molecule	Co	(1 1 1), cubic	0.85	10.3
Reduction to $3e^-$ per molecule and reoxidation	$PrCoO_3$	(2 2 0), cubic	0.35	27.1
Reduction to $3e^-$ per molecule, sintering in helium and reoxidation	$PrCoO_3$	(2 2 0), cubic	0.32	30.6
Reduction to $3e^-$ per molecule, sintering in helium and reoxidation	Pr_6O_{11}	(1 1 1), cubic	0.27	39.1
Reduction to $3e^-$ per molecule, sintering in helium and reoxidation	Co_3O_4	(3 1 1), cubic	0.40	23.1

*The apparatus correction was found to be $b = 0.17°$.
†For details see text.

in the former oxide the contracting sphere model (reduction to $1e^-$ per molecule) and the nucleation mechanism (reduction to $3e^-$ per molecule). Reduction of these perovskites up to 1000 K affects only the transition metal cation, Co^{3+}, since the rare-earth sesquioxides are not reducible at these temperatures [21]. These two reduction mechanisms have been observed in other transition metal oxides: for example $NiO \cdot SiO_2$ [22] and $NiO \cdot MoO_3$ [23] were found to exhibit a continuous decrease in the rate of reduction whereas unsupported NiO [24] and $NiO \cdot V_2O_5$ [25] yielded sigmoidal curves of reduction.

However, the XPS and the TPR results showed that $PrCoO_3$ is more easily reducible than $LaCoO_3$. This is in agreement with recent results indicating that the bond energy for Co–O in $PrCoO_3$ is lower than that in $LaCoO_3$ and also that the catalytic activity for oxidation of the former oxide is higher than that of the latter [3]. These results show a clear influence of the cation in the A position of the perovskite structure on the bulk and surface properties of these oxides. This effect may come from variations of the crystal cell dimensions which may in turn affect the Ln–O and Co–O interactions [3]. If this were the only factor to be considered, the reducibility and the catalytic activity of $LnCoO_3$ oxides should both exhibit a monotonous trend when passing from lanthanum to lutetium (the ionic radii of the 3^+ cations experience a continuous decrease from La^{3+} (0.115 nm) to Lu^{3+} (0.093 nm)). This hypothesis is not supported by the experimental evidence reported by Futai *et al.* [3]: the bond energy for Ln–O is a minimum and the catalytic activity for oxidation is a maximum for $EuCoO_3$ within the series of $LnCoO_3$ oxides. These results suggest that, besides geometric effects, the electronic structure $[Xe]4f^n5d^0$ of the rare-earth cations plays a certain role in the catalytic activity of these oxides, for oxidation and most probably for other reactions as well. Up to date the available literature studying the influence of the A cation in the chemical properties of perovskites is sparse. In order to gain a better understanding on this point more experimental information will be needed.

Acknowledgement

The authors are greatly indebted to the Spanish–North-American Joint Committee for Scientific and Technological Cooperation for sponsorship of this work.

References

1. Kh. M. MINACHEV, in Proceedings of 5th International Congress on Catalysis, Vol. 1, edited by J. W. Hightower (North-Holland, Amsterdam, 1973) p. 219.
2. Y. TAKASU, S. NISHIBE and Y. MATSUDA, *J. Catal.* **49** (1977) 236.
3. M. FUTAI, C. YONGHUA and LLHUI, *React. Kinet. Catal. Lett.* **31** (1986) 47.
4. T. ARAKAWA, N. OHARA and J. SHIOKAWA, *J. Mater. Sci.* **21** (1986) 1824.
5. J. M. D. TASCÓN and L. GONZÁLEZ TEJUCA, *React. Kinet. Catal. Lett.* **15** (1980) 185.
6. G. KREMENIĆ, J. M. L. NIETO, J. M. D. TASCÓN and L. GONZÁLEZ TEJUCA, *J. Chem. Soc., Faraday Trans. 1* **81** (1985) 939.
7. J. M. D. TASCÓN, S. MENDIOROZ and L. GONZÁLEZ TEJUCA, *Z. Phys. Chem. N.F.* **124** (1981) 109.
8. K. ICHIMURA, Y. INOUE and I. YASUMORI, *Bull. Chem. Soc. Jpn* **53** (1980) 3044.
9. E. A. LOMBARDO, K. TANAKA and I. TOYOSHIMA, *J. Catal.* **80** (1983) 340.
10. N. YAMAZOE, Y. TERAOKA and T. SEIYAMA, *Chem. Lett.* (1981) 1767.
11. J. L. G. FIERRO and L. GONZÁLEZ TEJUCA, *Appl. Surf. Sci.* **27** (1987) 453.
12. S. J. COCHRAN and F. P. LARKINS, *J. Chem. Soc., Faraday Trans. 1* **81** (1985) 2179.
13. L. GONZÁLEZ TEJUCA, A. T. BELL, J. L. G. FIERRO and M. A. PEÑA, *Appl. Surf. Sci.* in press.
14. T. NAKAMURA, G. PETZOW and L. J. GAUCKLER, *Mater. Res. Bull.* **14** (1979) 649.
15. M. CRESPIN and W. K. HALL, *J. Catal.* **69** (1981) 359.
16. J. L. G. FIERRO, J. M. D. TASCÓN and L. GONZÁLEZ TEJUCA, *ibid.* **93** (1985) 83.
17. M. CRESPIN, P. LEVITZ and L. GATINEAU, *J. Chem. Soc., Faraday Trans. 2* **79** (1983) 1181.
18. P. LEVITZ, M. CRESPIN and L. GATINEAU, *ibid.* **79** (1983) 1195.
19. N. W. HURST, S. J. GENTRY, A. JONES and B. D. McNICOL, *Catal. Rev.-Sci. Eng.* **24** (1982) 233.
20. C. J. KEATTCH and D. DOLLIMORE, in "An Introduction to Thermogravimetry", 2nd edn (Heyden, London, 1975) Ch. 5.
21. N. E. TOPP, in "Chemistry of the Rare-earth Elements" (Elsevier, Amsterdam, 1965).
22. A. ROMAN and B. DELMON, *Compt. Rend.* **C273** (1971) 1310.
23. A. I. VAGIN, N. V. BURMISTROVA and V. I. EROFEEV, *React. Kinet. Catal. Lett.* **28** (1985) 47.
24. R. HASEGAWA, *Trans. Natl. Res. Inst. Metall.* **20** (1978) 21.
25. M. POSPÍSIL, *J. Therm. Anal.* **27** (1983) 77.

Received 7 May
and accepted 22 July 1987